ROYAL SOCIETY OF CHEMISTRY

PAPER

Check for updates

Chiral cyanobiphenyl dimers – significance of the linking group for mesomorphic properties and helical induction†

Antonija Ožegović, [ID] [a] Jordan Hobbs, [ID] [b] Richard Mandle, [ID] [bc] Andreja Lesac [ID] [a] and Anamarija Knežević [ID] ⋆[a]

Cyanobiphenyl (CB) mesogenic molecules are a focal point in liquid crystal (LC) research and applications due to their chemical stability, ease of synthesis, broad mesophase temperature range, and other advantageous properties. The introduction of chirality into LC systems offers unique optical and mechanical properties with great potential, and exploring the CB building block in chiral LC dimers presents a promising avenue for further research. In this study, we present the synthesis of chiral and racemic dimers bearing a chiral center as part of their flexible spacer and two CB moieties at the ends, *i.e.* the first chiral CB dimers. The investigation includes ester and amide linking groups near the chiral center to evaluate the impact of molecular flexibility on mesomorphic behavior and helical twisting power (HTP). The synthesis of racemic and enantiomerically pure dimers enabled the comparison of their mesogenic properties. Our results revealed CB dimers bearing ester linking group exhibit rich nematic polymorphism, including the rarely obtained room-temperature twist-bend nematic (N_{TB}) phase. In contrast, the amide linking group suppresses LC properties but significantly enhances the HTP. These findings highlight the importance of intermolecular interactions and the balance of flexibility and rigidity near the chiral center in achieving desirable mesomorphic properties.

Introduction

Liquid crystals (LCs) are a state of matter between solid and liquid phases, combining the anisotropic properties of crystalline solids with the fluidity of liquids.[1] Among LC compounds, cyanobiphenyl (CB) LCs, first synthesized by George W. Gray in 1972,[2] are notable for their chemical stability, room-temperature nematic phases, wide temperature range for the nematic phase, large positive dielectric anisotropy, strong birefringence, *etc.* Given these beneficial properties, cyanobiphenyls (CBs) have found various applications in several areas of technology and fundamental research. Rod-shaped monomeric CBs, such as 5CB and 8CB, are commonly used in various LC applications due to their ease of experimentation at room temperature and commercial availability at a reasonable cost.[3] Likewise, in the field of LC dimers, the CB mesogenic unit plays a significant role.[4] LC dimers represent a notable group of LCs
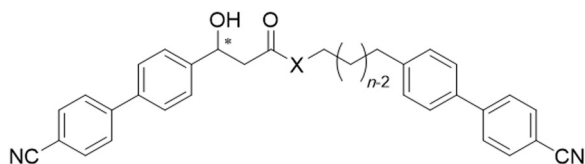
that consist of two mesogenic units connected by a flexible spacer.[5,6] Their unusual and rich mesomorphism differs from that of the corresponding monomers[4] and depends on the parity of the spacer.[5,7] Bent-shaped flexible dimers, owing their shape to an odd-numbered spacer, have gained a special interest due to the formation of the interesting twist-bend nematic (N_{TB}) phase.[8,9] Namely, LC dimers like CB7CB and CB9CB were among the first[9] and surely the most extensively studied mesogens that exhibit the N_{TB} phase.[10] This phase is particularly intriguing due to the spontaneous formation of chiral helical structures from achiral nematogens with an equal number of right- and left-handed helices.[8,10–12] The interest in the N_{TB} phase lies in its electro-optic response times which could be reduced to microseconds under the application of a DC field.[13,14] However, the potential use of this phase in electro-optic devices is limited given that the N–N_{TB} phase transition occurs well above the room-temperature in pure compounds. To date, only a few examples of a room temperature N_{TB} phase have been observed.[15,16]

When chirality is introduced into nematic LCs, helical organization is also induced, but with the particular handedness resulting in the chiral nematic phase.[17–20] This can be achieved by either incorporating a chiral moiety within the molecular structure of the LC or by adding mesogenic or non-

[a] Ruđer Bošković Institute, Bijenička 54, 10000 Zagreb, Croatia.
  E-mail: anamarija.knezevic@irb.hr
[b] School of Physics and Astronomy, University of Leeds, Leeds LS2 9JT, UK
[c] School of Chemistry, University of Leeds, Leeds LS2 9JT, UK

† Electronic supplementary information (ESI) available. See DOI: https://doi.org/10.1039/d4tc02597k

Compound	n	X	Stereochemistry
CBCOO5CB	5	O	rac
CBCOO7CB	7	O	rac
CBCONH5CB	5	NH	rac
CBCONH7CB	7	NH	rac
S-CBCOO5CB	5	O	S
S-CBCOO7CB	7	O	S
S-CBCONH5CB	5	NH	S
S-CBCONH7CB	7	NH	S

Fig. 1 Structures of prepared cyanobiphenyl (CB) LC dimers.

mesogenic chiral dopants to the achiral LC host.[21] The helical superstructure, characterized by the magnitude and sign of the helical pitch P, possesses desirable properties, such as selective light reflection and responsiveness to external electric field, that have been utilized in various applications ranging from development of optical sensors to smart windows, and other technologies.[19,20,22] Furthermore, chiral mesogenic molecules can exhibit other chiral LC phases including chiral smectics, frustrated phases like twist grain boundary (TGB) and blue phases (BP), or chiral N_{TB} phase (N^*_{TB}).[18] The N^*_{TB} phase, the most recently discovered, appears to be thermodynamically equivalent to the conventional N_{TB} phase, despite their markedly different optical textures. To date, N^*_{TB} has been observed in only a handful of chiral dimeric materials.[23–27] Among these studies, only recent ones report series of chiral and racemic LC dimers and provide a comparison between the N_{TB} and N^*_{TB} phases.[25–27]

Chiral rod-shaped LCs containing CB building block have been developed following their achiral analogues.[28,29] However, in the case of chiral LC dimers, the CB building block was commonly used only in the achiral part of the molecule and not located near the chiral center,[26,30,31] regardless of whether the chiral moiety was located in the terminal chain, mesogenic unit or the flexible spacer. A chiral dimer bearing two CB moieties at the ends, as an analogue of CBnCB dimers, has not been synthesized so far.

Recently, we reported on the use of the chiral 3-aryl-3-hydroxypropanoic ester subunit as a versatile chiral building block for the preparation of novel LC compounds, both in racemic and enantiomerically pure forms.[32] This building block possess a less bulky hydroxyl group compared to methyl usually used for generating the stereogenic center in LCs.[17] In this paper, we prepared 3-cyanobiphenyl-3-hydroxypropanoic ester, which was used for the preparation of the first chiral

CB dimers featuring a chiral center as part of their flexible spacer (Fig. 1). By synthesizing enantiomerically pure and racemic dimers, we were able to compare the mesomorphic behavior of both forms. Ester and amide linking groups were incorporated near the chiral center to investigate the effect of molecular flexibility/rigidity on the mesomorphic behavior and helical twisting power (HTP). While CB dimers bearing ester linking group exhibit rich nematic polymorphism, including room-temperature N_{TB} phase, in combination with low HTP, amide linking group suppresses LC properties and strongly enhances the HTP.

Results and discussion

Synthesis of LCs

The targeted molecules were prepared following the convergent synthetic route from 3-((tert-butyldimethylsilyl)oxy)-3-(4′-cyano-[1,1′-biphenyl]-4-yl)propanoic acid, in both racemic (**1**) and enantiomerically pure (**S-1**) form, in combination with the corresponding cyanobiphenyl alcohols (**2a**, **2b**) and cyanobiphenyl amines (**3a**, **3b**) (Scheme 1). Esterification of acids with alcohols provided four TBS-protected esters (**4a**, **4b**, **S-4a** and **S-4b**), while amidation of acids with amines provided four TBS-protected amides (**5a**, **5b**, **S-5a** and **S-5b**). The targeted LC esters (**CBCOO5CB**, **CBCOO7CB**, **S-CBCOO5CB**, and **S-CBCOO7CB**) and amides (**CBCONH5CB**, **CBCONH7CB**, **S-CBCONH5CB** and **S-CBCONH7CB**) were obtained by removing the tert-butyl-dimethylsilyl protection in 75% to 93% yields.
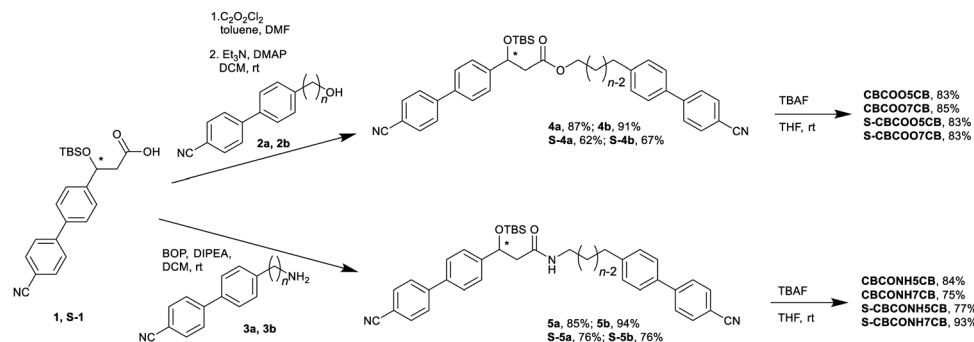
The crucial intermediate acid **1** was synthesized starting from 4-bromobenzaldehyde according to the analogous synthetic procedure reported previously (Scheme 2).[27,32] Both racemic (**1**) and enantiopure forms (**S-1**) were prepared, enabling the preparation of racemic and enantiopure final LC compounds. The absolute configuration of the generated chiral center in product's chiral acid was presumed to be (S), given that it was unambiguously confirmed for previously reported analogous compounds.[32]

Mesomorphic behaviour

The thermal behavior of compounds bearing 3-cyanobiphenyl-3-hydroxypropanoic ester and amide subunit is shown in Fig. 2 and Table S1 (ESI†). All racemic compounds (**CBCOO5CB**, **CBCOO7CB**, **CBCONH5CB** and **CBCONH7CB**) and chiral esters (**S-CBCOO5CB**, **S-CBCOO7CB**) are mesogenic, while chiral amides (**S-CBCONH5CB**, **S-CBCONH7CB**) crystallize quickly from the isotropic melt, and LC phases are not observed.

In general, esters exhibit more extensive mesomorphic behavior, which is suppressed in amides presumably due to stronger interactions resulting from the presence of hydrogen bonding.[33] As a result, the differences in mesogenic properties are tremendous. The transition temperatures of prepared esters, both racemic (**CBCOO5CB** and **CBCOO7CB**) and chiral (**S-CBCOO5CB** and **S-CBCOO7CB**), are lower compared to previously reported achiral CBnCB compounds.[34] This is expected since the introduction of the stereogenic center introduces

13986 | J. Mater. Chem. C, 2024, **12**, 13985–13993

This journal is © The Royal Society of Chemistry 2024

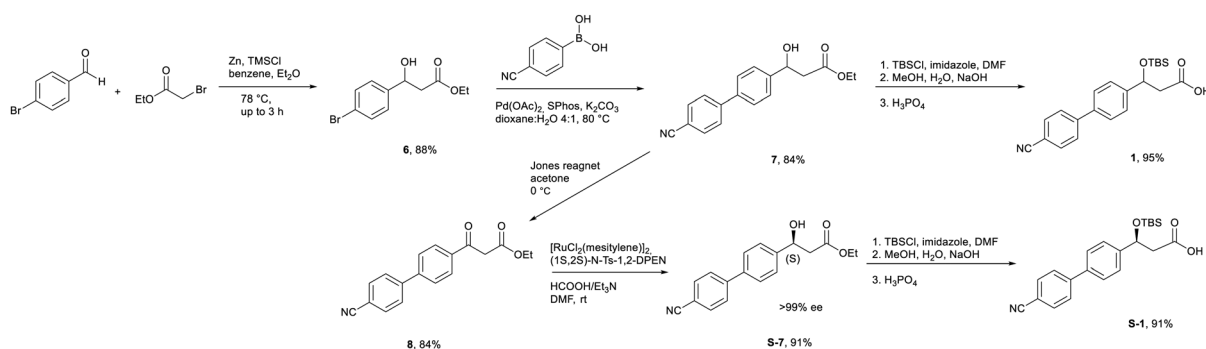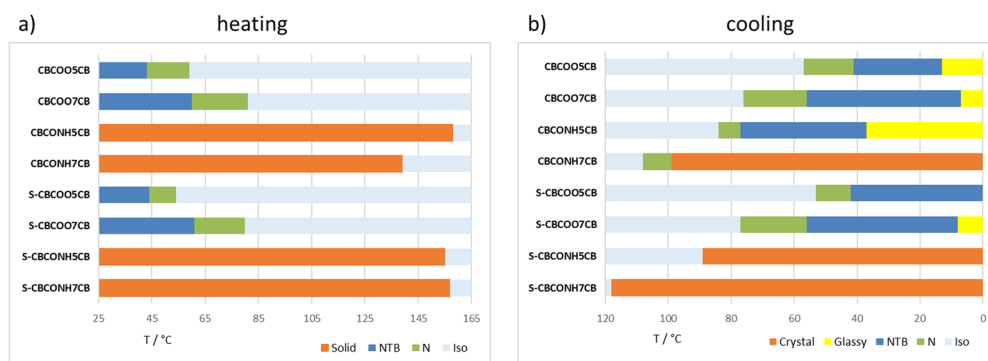Scheme 1 Synthesis of CB LC dimers.

Scheme 2 Synthesis of racemic and enantiomerically pure intermediate acids **1** and **S-1**.

Fig. 2 Transition temperatures (°C) for the synthesized compounds obtained in (a) heating and (b) cooling.

branching in the structure, resulting in the lowering of transition temperatures. In contrast, the clearing points of amide homologues are higher compared to esters (Fig. 2), which is presumably the consequence of the presence of strong hydrogen bonding in amides.[35] Comparing the chiral materials to racemates, there is only minimal difference in the mesophase stability for the ester series, which is in agreement with previously reported findings for structurally similar LC dimers.[27] In contrast, in chiral amides crystallization at higher temperatures than for the racemates completely suppresses the occurrence of LC phases.

The prepared chiral and racemic esters exhibit nematic polymorphism, including enantiotropic, room-temperature twist-bend nematic (N_{TB}) phases. Upon cooling or prolonged standing, they undergo a transition into a glassy state, a feature highly valued for potential new applications.[16,36] The elongation of the spacer from five methylene units in compounds **CBCOO5CB** and **S-CBCOO5CB** to seven in **CBCOO7CB** and **S-CBCOO7CB** stabilizes the LC phases which is observed in higher transition temperatures. Racemic ester homologs exhibit typical mesophases observed in odd-membered achiral dimers,[4] *i.e.* nematic and N_{TB} phases. The nematic phases of racemic homologs **CBCOO5CB** and **CBCOO7CB** were identified by their distinctive optical textures. The uniaxial nematic phase was identified according to its typical schlieren texture (Fig. 3a). On cooling, the transition from N to N_{TB} showed a characteristic blocky texture (Fig. 3b), from which the rope texture developed

This journal is © The Royal Society of Chemistry 2024
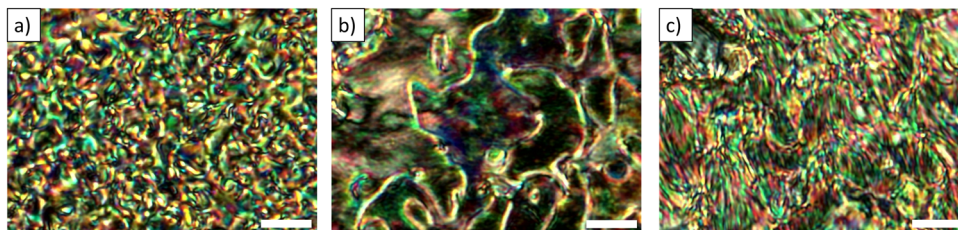
J. Mater. Chem. C, 2024, **12**, 13985–13993 | **13987**

Fig. 3 Optical textures of **CBCOO5CB** obtained on cooling. (a) The schlieren texture of the N phase at 56 °C. (b) The blocky texture of the N_{TB} at 41 °C. (c) The rope texture of the N_{TB} phase at 28 °C. The scale bar is 10 μm.

(Fig. 3c). Indeed, the analysis of unaligned two-dimensional SAXS/WAXS patterns of compound **CBCOO7CB** confirmed the phase identification. The 2D SAXS patterns in the nematic and N_{TB} phases feature only weak diffuse scattering at small angles, refuting the possibility of smectic/lamellar order and supporting our phase identification as N and N_{TB} (Fig. 4). The low intensity of the SAXS peak is likely due to the symmetric nature of the mesogenic group which allows the molecules to act almost chain like giving little variation in electron density across the ends of the molecules and resulting in low contrast for X-ray scattering.[37,38] The position of the wide angle peak shifts slightly on cooling as a result of the molecules adopting a heliconical structure and consistent with prior results.[39] The 2D SAXS patterns remain unchanged even at

−10 °C which supports the results obtained by DSC where crystallization was not observed (Table S1 and Fig. S1, ESI†).

Upon heating **S-CBCOO5CB** and **S-CBCOO7CB**, both compounds reveal the typical texture characteristic of the N* phase (Fig. 5a) before the clearing temperature. However, upon cooling from the isotropic liquid, this phase appears almost completely black without any texture (Fig. 5b) and becomes dark blue near the transition to the lower temperature LC phase. Only by applying mechanical stress, a small fingerprint texture appears within the bluish background (Fig. 5c). Upon further cooling, another mesophase appears with a variety of textures depending on the cooling rate and the alignment of the sample (Fig. 6). By analogy with the mesophase behavior of racemic analogs and previously observed textures of similar compounds,[27] the low-temperature phase corresponds to the chiral N_{TB}^{*} phase. Furthermore, the phase identification as N* and N_{TB}^{*} was further supported by X-ray scattering studies on compound **S-CBCOO7CB** (Fig. S2, ESI†). The texture remains unchanged upon cooling to room temperature or upon fast cooling below room temperature. DSC thermograms reveal a transition to the glass phase below room temperature (Fig. S3, ESI†).

The mesomorphic behavior of the racemic (**CBCONH5CB** and **CBCONH7CB**) and chiral (**S-CBCONH5CB** and **S-CBCONH7CB**) amide dimers show greater dependence on spacer length and enantiomeric purity. Incorporation of the amide group in the molecular structure is known to have a detrimental effect on mesogenic properties.[33] However, secondary amides can form LC phases with high melting points attributed to the presence of strong hydrogen bonding.[33,35,40] Racemic compound **CBCONH5CB** exhibits monotropic nematic phases upon cooling (Fig. 2 and Table S1, ESI†). The large supercooling effect reveals the transition from isotropic to nematic phase at 84 °C, even though the melting point is at 160 °C. The nematic phase, characterized by a typical thread-like texture (Fig. 7a), changes to the N_{TB} phase upon further cooling at 77 °C (Fig. 7b). The texture of the N_{TB} phase changes upon annealing at the constant temperature (Fig. 7c) and begins to resemble the texture of the N_{TB}^{*} phase of chiral esters (Fig. 6). Upon further standing, slow crystallization begins at various locations on the sample (Fig. 7d). The elongation of the spacer slightly lowers the clearing point (Fig. 2), raises the transition temperatures, and suppresses the formation of the N_{TB} phase due to fast crystallization. Upon cooling longer racemic analogue **CBCONH7CB**, the nematic phase appears at 109 °C with fast crystallization preceding at 99 °C or even at higher temperatures over time (Fig. S4, ESI†).
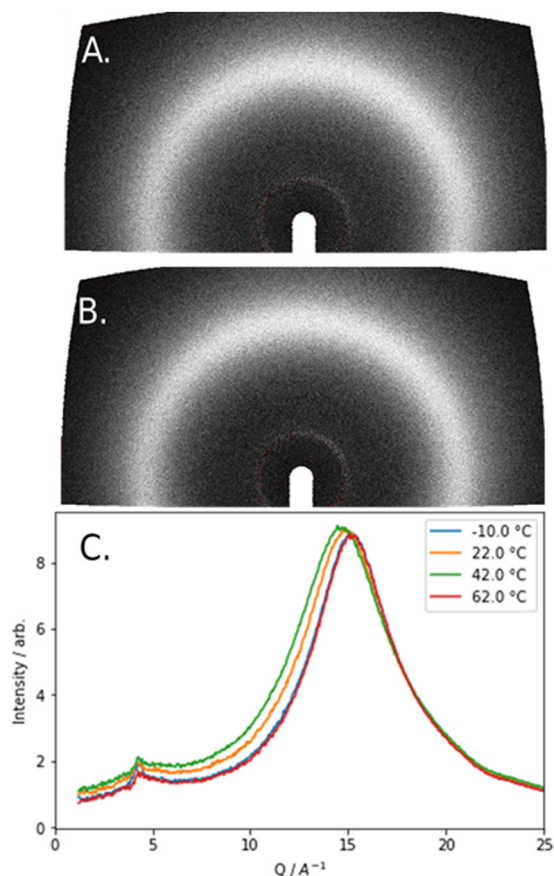

Fig. 4 2D SAXS patterns for (A) **CBCOO7CB** in the nematic phase at 50 °C; (B) **CBCOO7CB** in the N_{TB} phase at 30 °C. (C) plot of integrated scattering intensity *versus* Q at a range of temperatures.

13988 | *J. Mater. Chem. C*, 2024, **12**, 13985–13993

This journal is © The Royal Society of Chemistry 2024

Fig. 5 Optical textures of **S-CBCOO7CB** in the N* phase. (a) The texture of the N* phase at 68 °C obtained on heating in a planar 5 μm cell. (b) The texture of the N* phase at 57 °C obtained on cooling in a planar 5 μm cell. (c) The texture of the N* phase at 70 °C obtained on cooling and under mechanical stress. The scale bar is 20 μm.
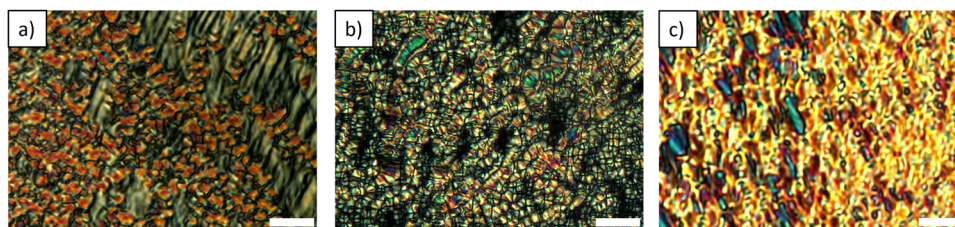

Fig. 6 Optical textures of **S-CBCOO7CB** in the N_{TB}^* phase obtained on cooling in a 5 μm planar cell at various cooling rates and at different locations on the sample. (a) The texture at 55 °C. (b) The texture at 50 °C. (c) The texture at 43 °C. The scale bar is 10 μm.
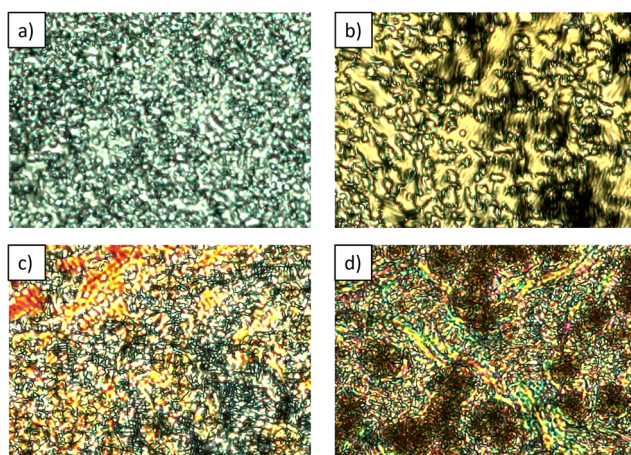

Fig. 7 Optical textures of **CBCONH5CB** obtained on cooling. (a) The thread-like texture of the N phase at 79 °C. (b) The blocky texture of the N_{TB} at 71 °C. (c) Texture of the N_{TB} phase at 71 °C upon standing. (d) Texture of the N_{TB} phase and crystallization occurring at 58 °C. The scale bar is 10 μm.

Fig. 8 Histogram plots of the probability of a given bend angle for **S-CBCOO7CB** and **S-CBCONH7CB**. Conformers were generated and processed as described in the text.

Both chiral compounds (**S-CBCONH5CB** and **S-CBCONH7CB**) crystalize very quickly upon cooling, which prevents the chiral nematic phase from forming. Furthermore, depending on the cooling rate and on the number of thermal cycles, different crystal phases occur, which is evident both using POM (Fig. S5, ESI†) and DSC (Fig. S6, ESI†).

We studied the conformational preferences of compounds **S-CBCOO7CB** and **S-CBCONH7CB** by generating 2048 conformers for each system followed by geometry optimization of each conformer. After removing duplicate entries, we calculated the bend-angle of eac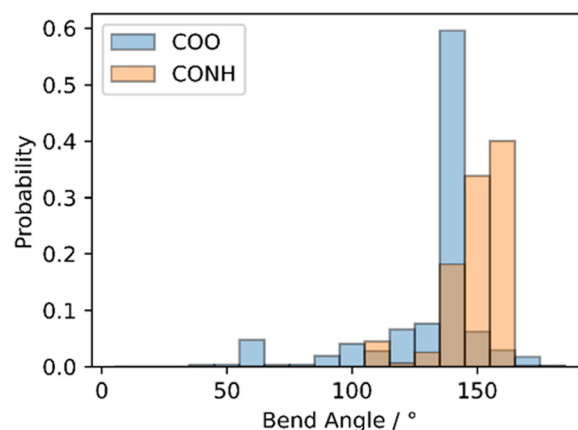h unique conformer as the angle between the vectors defined by the two nitrile C–N bonds. From the energy of each conformer, we then obtain the probability weighted bend-angle calculated at a temperature of 298 K (Fig. 8). The two materials are not especially different in this regard: both having a gross bent-shape. Overall, amide linking group results in higher probability of conformers with larger bend-angle compared to ester linking group, *i.e.* it confers a preference for extended conformations for the amide **S-CBCONH7CB**. These extended conformers are then well positioned for further intermolecular hydrogen bonding interactions which is the likely cause of the elevated melting point and limited supercooling range experienced by these materials.

Given that the bulky methyl group in the spacer of bent-shaped dimers is known to reduce lateral intermolecular

This journal is © The Royal Society of Chemistry 2024

J. Mater. Chem. C, 2024, **12**, 13985–13993 | **13989**

interactions and completely suppress mesogenic properties,[24] the hydroxyl group proved to be a good choice in constructing the stereogenic center. The amide-linked compounds exhibit relatively high melting points resulting in reduced mesogenic properties that are completely lost in combination with high enantiomeric purity. At the same time, CB dimers bearing an ester linking group exhibit interesting nematic polymorphism – both racemic and chiral compounds generate nematic and twist-bend nematic phases at relatively low temperatures. Interestingly, CB dimers bearing a stereogenic center are room-temperature N_{TB} nematics, representing one of the rare examples of such materials. Additionally, upon further cooling or prolonged standing, these LC compounds enter the glass state, preserving the texture of the N_{TB} phase.

Helical twisting power of prepared LC dimers

Adding chiral dopants to the LC material is a more commonly used method to obtain chiral LC phases since it requires only a small amount of chiral material. The efficiency of a chiral dopant in inducing helical organization in the nematic phase is quantified by the "helical twisting power" (HTP). HTP is defined as $\beta = 1/Pcr$, where P (μm) is the pitch of the chiral nematic phase, c is the molar fraction of the dopant in the

nematic host, and r is its optical purity.[17] The right- or left-handedness of the helix is designed by the positive or negative sign of the HTP, respectively, and was determined directly from the wedge cells applying Gerber's rule.[41]

To investigate the effect of linking group and spacer length of prepared chiral CB dimers on chiral induction, we determined the HTP in the nematic hosts for all four chiral dimers. We chose as hosts two nematic solvents that are typical commercial rod-shaped nematogens, 5CB and 6OCB, as well as a bent-shaped dimer BNA-76,[42] which allowed us to study the effect of a host shape (Fig. 9a).

The difference in HTP values between esters (**S-CBCOO5CB**, **S-CBCOO7CB**) and amides (**S-CBCONH5CB**, **S-CBCONH7CB**) is significant in all hosts (Fig. 9b and Table S2, ESI†), while the differences in respect to the spacer length are minor. The HTP values of esters in all hosts are quite low (β = 0.7–4 μm^{-1}). On the contrary, much higher HTPs are observed for amide dimers, which is rarely the case for molecules owing their chirality to a single stereogenic center.[43] In a bent-shaped dimer host (BNA-76), the HTP values of both amides are moderate (β = 9–10 μm^{-1}), whilst in rod-shaped hosts amides are strong inducers of the chiral nematic phase (β = 24–34 μm^{-1}). A left-handed helix is observed in most of the dopant–host
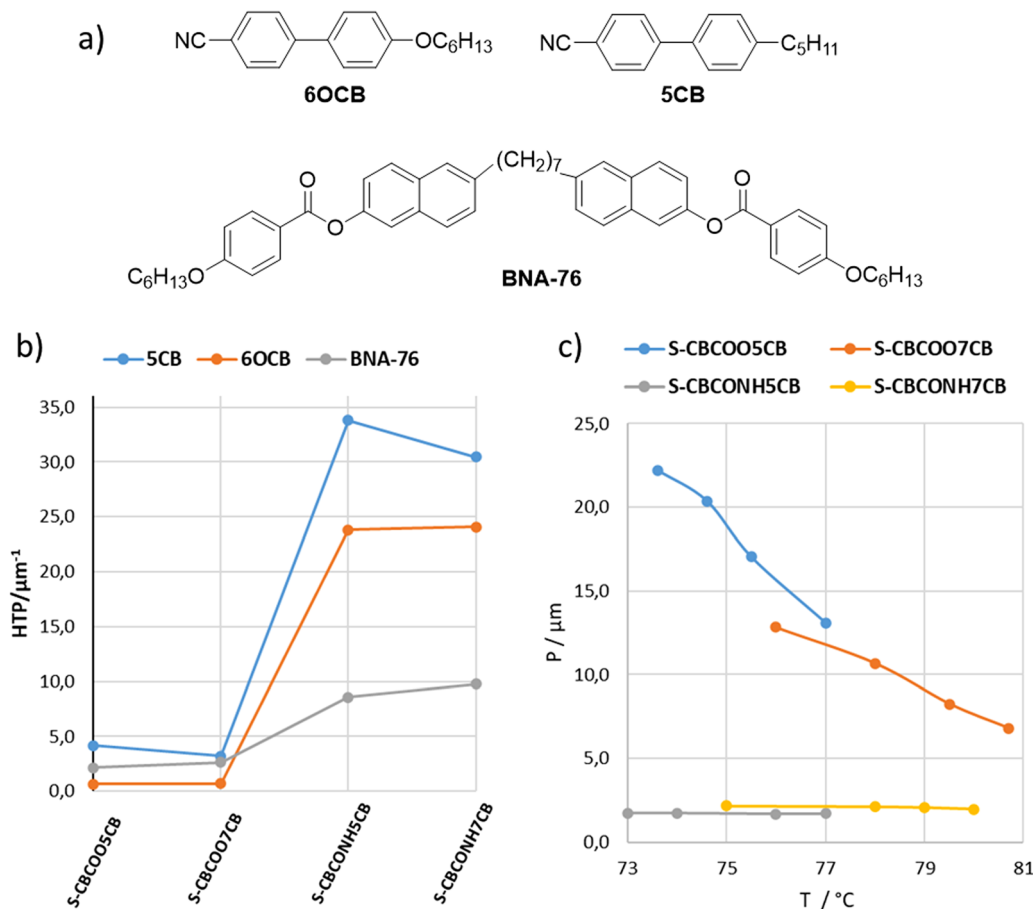

Fig. 9 (a) Chemical structure of the nematic host compounds. (b) HTP of the chiral CB dimers doped in 5CB, 6OCB, and BNA-76. (c) Temperature dependence of the pitch (P/μm) of prepared chiral compounds in 6OCB.

13990 | *J. Mater. Chem. C*, 2024, **12**, 13985–13993

This journal is © The Royal Society of Chemistry 2024

combinations, with the exception of both esters in 5-CB where a right-handed helix was observed.

The value of HTP of chiral dopants depends on the molecular shape and anisometry of the dopant, *i.e.*, its preferential conformers, the distance of the chiral center from the rigid aromatic core, the type of chemical bonds, and specific intermolecular interactions of the dopant with the host.[43–45] The distance between the stereogenic center and the rigid mesogenic core within a chiral molecule is important – the pitch length decreases, and the HTP therefore increases, the closer the stereogenic center is positioned to the mesogenic core.[24,29] The HTP values of esters correspond to the HTP values of analogous LC molecules bearing a phenyl moiety near the chiral center[27] and are higher than for dimers bearing the chiral center on the second position to the aromatic core.[24] However, in both esters and amides, the stereogenic center is positioned next to the rigid aromatic core, which reduces its conformational freedom and should contribute to shortening the pitch length of the chiral nematic phase. Since esters and amides exhibit quite different HTPs, the results indicate that the proximity of the chiral center to the mesogenic unit is not a dominant effect in obtaining high HTP. Besides the similarity in the chemical structure between the chiral dopant and the nematic host,[45] the important characteristic is the flexibility of the dopant molecule, especially the flexibility near the stereogenic center. In general, molecules with reduced flexibility have stronger twisting ability, while flexibility is associated with a decrease in the HTP.[24,43] In amides, the flexibility is severely reduced compared to esters due to restricted rotation around the C–N bond.[46,47] In fact, the stereogenic center is located in the spacer, surrounded by a rigid aromatic core on one side and a rigid amide bond on the other. This position severely reduces the flexibility of the stereogenic center (Fig. S7, ESI†), which in combination with extended molecular shape (Fig. 8), presumably leads to high HTP.

The temperature dependance of the induced helical pitch is also remarkably different in the case of esters and amides (Fig. 9c and Table S3, ESI†). In the case of esters *S*-CBCOO5CB and *S*-CBCOO7CB the temperature dependance of helical pitch is inconsistent both in direction and magnitude, and highly depends on the host. In 5CB, helical pitch slightly decreases upon lowering the temperature, while in the structurally very similar host 6OCB a dramatical increase of the pitch is observed. When the host is the bent-shape dimer BNA-76, the increase in the pitch is evident but not as significant. In contrast, the helical pitch of the mixtures with amides *S*-CBCONH5CB and *S*-CBCONH7CB is more straightforward and less temperature dependent – it only slightly increases in all hosts. In most cases, the cholesteric pitch decreases upon increasing temperature, which is nowadays used in technological applications.[18,48] However, this dependance can differ in some cases, and various factors have been discussed to be responsible for the temperature dependance of the helical pitch, including the temperature dependence of the concentration ratios of conformers with presumably different HTP for flexible dimers, the temperature dependance of elastic constants of selected nematic host,

the peculiarities of the conformational structure around the chiral center of the dopant, *etc.*[49,50] The difference in rigidity of amides and esters (Fig. S7, ESI†), and consequently their different interactions with the nematic host reflect on the temperature dependance of the pitch.

Experimental

Synthesis

The targeted compounds were prepared both in racemic and in enantiomerically pure forms. Compounds **2a** and **2b** were prepared according to literature procedure.[51] Synthetic procedures and chemical characterization of intermediate compounds and final LC dimers are given in the accompanying ESI.†

Characterization of the LC properties

The liquid crystalline behavior of all final materials was analyzed by a combination of polarized optical microscopy (POM), differential scanning calorimetry (DSC) and X-ray diffraction. The list and description of all instrumentation and characterization methods used in this work is provided in the ESI.†

Determination of the helical pitch

The helical pitch of enantiomerically pure compounds and mixtures of the compounds in three nematic hosts, namely 4-cyano-4′-pentylbiphenyl (5CB), 4′-hexyloxy-4-cyanobipheny (6OCB) and 1,7-bis(6-(4-hexyloxybenzoyloxy)naphthalene-2-yl)-heptane (BNA-76)[42] was determined by the Cano-wedge method using commercial EHC cells (KCRS-5, $\tan \theta = 0.0192$). The helical twist sense was determined directly from the wedge cells by applying Gerber's rule.[41]

Computational methods

Conformational preferences of compounds *S*-CBCOO7CB and *S*-CBCONH7CB were studied by generating 2048 conformers for each system using the ETKDGv3 (Experimental-Torsion with Knowledge Distance Geometry version 3) as implemented in RDkit.[52–55] The geometry of each conformer was then optimized with the PM7 semi-empirical method[56] as implemented in Gaussian G16.[57] After removing duplicate entries, *e.g.* cases where the optimization of two different conformers converge to identical geometries, the bend-angle of each unique conformer was calculated as the angle between the vectors defined by the two nitrile C–N bonds. From the energy of each conformer, the probability weighted bend-angle calculated at a temperature of 298 K was obtained.

Conclusion

This article describes the synthesis and mesomorphic properties of the first chiral LC dimer bearing two cyanobiphenyl (CB) moieties at the ends. The hydroxyl group was successfully incorporated into the flexible spacer of the LC dimer, generating a chiral center without suppressing mesogenic properties.

This journal is © The Royal Society of Chemistry 2024

J. Mater. Chem. C, 2024, **12**, 13985–13993 | **13991**

The dimers, which differ in spacer length and the linking group near the chiral center, were prepared in both racemic and enantiomerically pure forms, allowing for a comparative study of the resulting mesophases. The importance of a linking group on molecular flexibility, intermolecular interactions and consequently on mesogenic properties and chiral induction in nematic host were confirmed by comparing homologues bearing the ester and amide linking group. Notably, dimers with an ester linking group exhibit interesting nematic polymorphism including enantiotropic, room-temperature N_{TB} phases in both racemic and chiral compounds, representing a rare example of such materials. On the other hand, amide-linked dimers display suppressed mesogenic properties due to hydrogen bonding, which are completely lost when combined with high enantiomeric purity. However, amide dimers exhibit significantly higher helical twisting power (HTP), indicating that reduced flexibility near the stereogenic center enhances chiral induction. This study demonstrates an inverse correlation between mesogenic properties and chirality transfer: molecules with lower flexibility lack mesogenic properties but significantly influence chirality induction. The synthesized molecules show great potential for further research and applications due to their unique properties – favorable temperature range and enantiomeric purity in combination with simple synthetic approach. Chiral amides open possibilities for new synthetically easily accessible amides with potentially high HTPs, including monomer LCs. The room-temperature N_{TB} phase, obtained by both chiral and racemic ester-linked CB dimers, paws a way for fundamental research on the N_{TB} phase. Moreover, it represents a step towards potential applications in the field of electro-optics, given the benefits of its structure containing the cyanobiphenyl unit combined with a favorable temperature operating range.

Data availability

The data supporting this article have been included as part of the ESI.†

Conflicts of interest

There are no conflicts to declare.

Acknowledgements

References

1 J. W. G. Goodby, *Handbook of liquid crystals*, Wiley-VCH Verlag, Weinheim, Germany, 2nd edn, 2014.
2 D. A. Dunmur, *Liq. Cryst.*, 2015, 1–10.
3 J. P. F. Lagerwall, *Liq. Cryst.*, 2023, 1–15.
4 C. T. Imrie, R. Walker, J. M. D. Storey, E. Gorecka and D. Pociecha, *Crystals*, 2022, **12**, 1245.
5 C. T. Imrie and P. A. Henderson, *Chem. Soc. Rev.*, 2007, **36**, 2096.
6 S. K. Pal and S. Kumar, *Liquid crystal dimers*, Cambridge University Press, Cambridge, 2017.
7 A. Jakli, *Liq. Cryst.*, 2022, **49**, 1010–1019.
8 I. Dozov, *Europhys. Lett.*, 2001, **56**, 247–253.
9 M. Cestari, S. Diez-Berart, D. A. Dunmur, A. Ferrarini, M. R. De La Fuente, D. J. B. Jackson, D. O. Lopez, G. R. Luckhurst, M. A. Perez-Jubindo, R. M. Richardson, J. Salud, B. A. Timimi and H. Zimmermann, *Phys. Rev. E: Stat., Nonlinear, Soft Matter Phys.*, 2011, **84**, 031704.
10 R. J. Mandle, *Molecules*, 2022, **27**, 2689.
11 C. Tschierske, *Liq. Cryst.*, 2018, **45**, 2221–2252.
12 M. Šepelj, A. Lesac, U. Baumeister, S. Diele, H. L. Nguyen and D. W. Bruce, *J. Mater. Chem.*, 2007, **17**, 1154–1165.
13 V. P. Panov, R. Balachandran, M. Nagaraj, J. K. Vij, M. G. Tamba, A. Kohlmeier and G. H. Mehl, *Appl. Phys. Lett.*, 2011, **99**, 261903.
14 C. Meyer, G. R. Luckhurst and I. Dozov, *Phys. Rev. Lett.*, 2013, **111**, 067801.
15 Y. Wang, G. Singh, D. M. Agra-Kooijman, M. Gao, H. K. Bisoyi, C. Xue, M. R. Fisch, S. Kumar and Q. Li, *CrystEngComm*, 2015, **17**, 2778–2782.
16 Y. Arakawa, K. Komatsu, T. Shiba and H. Tsuji, *Mater. Adv.*, 2021, **2**, 1760–1773.
17 in *Chirality in Liquid Crystals*, ed. H.-S. Kitzerow and C. Bahr, Springer-Verlag, New York, 2001.
18 I. Dierking, *Symmetry*, 2014, **6**, 444–472.
19 H. K. Bisoyi and Q. Li, *Chem. Rev.*, 2022, **122**, 4887–4926.
20 K. Ariga, T. Mori, T. Kitao and T. Uemura, *Adv. Mater.*, 2020, **32**, 1905657.
21 R. Eelkema and B. L. Feringa, *Org. Biomol. Chem.*, 2006, **4**, 3729–3745.
22 P. Cachelin, J. P. Green, T. Peijs, M. Heeney and C. W. M. Bastiaansen, *Adv. Opt. Mater.*, 2016, **4**, 592–596.
23 E. Gorecka, N. Vaupotič, A. Zep, D. Pociecha, J. Yoshioka, J. Yamamoto and H. Takezoe, *Angew. Chem., Int. Ed.*, 2015, **54**, 10155–10159.
24 R. J. Mandle and J. W. Goodby, *RSC Adv.*, 2018, **8**, 18542–18548.
25 R. Walker, D. Pociecha, J. M. D. Storey, E. Gorecka and C. T. Imrie, *Chem. – Eur. J.*, 2019, **25**, 13329–13335.

13992 | *J. Mater. Chem. C*, 2024, **12**, 13985–13993

This journal is © The Royal Society of Chemistry 2024

26 R. Walker, D. Pociecha, M. Salamonczyk, J. M. D. Storey, E. Gorecka and C. T. Imrie, *ChemPhysChem*, 2023, **24**, e202200807.

27 A. Ožegović, A. Knežević, J. Novak, S. Šegota, P. Davidson and A. Lesac, *ChemPhysChem*, 2024, e202400065.

28 G. W. Gray and D. G. McDonnell, *Electron. Lett.*, 1975, **11**, 556.

29 G. W. Gray and D. G. McDonnell, *Mol. Cryst. Liq. Cryst.*, 1976, **37**, 189–211.

30 A. E. Blatch, I. D. Fletcher and G. R. Luckhurst, *J. Mater. Chem.*, 1997, **7**, 9–17.

31 C. V. Yelamaggad, G. Shanker, U. S. Hiremath and S. Krishna Prasad, *J. Mater. Chem.*, 2008, **18**, 2927.

32 I. Dokli, A. Ožegović, A. Šimanović, M. Hromin, A. Knežević, A. Višnjevac and A. Lesac, *J. Org. Chem.*, 2022, **87**, 14045–14057.

33 G. J. Strachan, W. T. A. Harrison, J. M. D. Storey and C. T. Imrie, *Phys. Chem. Chem. Phys.*, 2021, **23**, 12600–12611.

34 D. A. Paterson, J. P. Abberley, W. T. Harrison, J. M. Storey and C. T. Imrie, *Liq. Cryst.*, 2017, 1–20.

35 R. A. Vora and R. Gupta, *Mol. Cryst. Liq. Cryst.*, 1981, **67**, 215–220.

36 Y. Arakawa, Y. Ishida and H. Tsuji, *Chem. – Eur. J.*, 2020, **26**, 3767–3775.

37 M. R. Tuchband, M. Shuai, K. A. Graber, D. Chen, C. Zhu, L. Radzihovsky, A. Klittnick, L. M. Foley, A. Scarbrough, J. H. Porada, M. Moran, J. Yelk, D. Bedrov, E. Korblova, D. M. Walba, A. Hexemer, J. E. Maclennan, M. A. Glaser and N. A. Clark, *arXiv*, 2017, preprint, arXiv:1703.10787, DOI: **10.48550/arXiv.1703.10787**.

38 M. R. Tuchband, D. A. Paterson, M. Salamończyk, V. A. Norman, A. N. Scarbrough, E. Forsyth, E. Garcia, C. Wang, J. M. D. Storey, D. M. Walba, S. Sprunt, A. Jákli, C. Zhu, C. T. Imrie and N. A. Clark, *Proc. Natl. Acad. Sci. U. S. A.*, 2019, **116**, 10698–10704.

39 R. J. Mandle and J. W. Goodby, *Phys. Chem. Chem. Phys.*, 2019, **21**, 6839–6843.

40 G. J. Strachan, M. M. Majewska, D. Pociecha, J. M. D. Storey and C. T. Imrie, *ChemPhysChem*, 2023, **24**, e202200758.

41 P. R. Gerber, *Z. Naturforsch., A: Phys. Sci.*, 1980, **35**, 619–622.

42 A. Knežević, M. Sapunar, A. Buljan, I. Dokli, Z. Hameršak, D. Kontrec and A. Lesac, *Soft Matter*, 2018, **14**, 8466–8474.

43 S. Pieraccini, S. Masiero, A. Ferrarini and G. Piero Spada, *Chem. Soc. Rev.*, 2011, **40**, 258–271.

44 A. Kozachenko, V. Nazarenko, V. Sorokin, V. Tishchenko, Y. Tishchenko and S. Vakhnin, *Mol. Cryst. Liq. Cryst. Sci. Technol., Sect. A*, 1998, **324**, 251–256.

45 K. Fukuda, H. Suzuki, J. Ni, M. Tokita and J. Watanabe, *Jpn. J. Appl. Phys.*, 2007, **46**, 5208.

46 J. F. Liebman and A. Greenberg, *Biophys. Chem.*, 1974, **1**, 222–226.

47 C. R. Kemnitz and M. J. Loewen, *J. Am. Chem. Soc.*, 2007, **129**, 2521–2528.

48 T. J. White, M. E. McConney and T. J. Bunning, *J. Mater. Chem.*, 2010, **20**, 9832.

49 N. I. Shkolnikova, L. A. Kutulya, N. S. Pivnenko, R. I. Zubatyuk and O. V. Shishkin, *Crystallogr. Rep.*, 2005, **50**, 1005–1011.

50 N. I. Shkolnikova, L. A. Kutulya, N. S. Pivnenko, A. D. Roshal and G. P. Semenkova, *Liq. Cryst.*, 2007, **34**, 1193–1200.

51 K. Wang, M. Jirka, P. Rai, R. J. Twieg, T. Szilvási, H. Yu, N. L. Abbott and M. Mavrikakis, *Liq. Cryst.*, 2019, **46**, 397–407.

52 J. L. Hobbs, C. J. Gibb, E. Cruickshank, R. Walker and R. J. Mandle, *Liq. Cryst.*, 2024, 1–13.

53 S. Wang, J. Witek, G. A. Landrum and S. Riniker, *J. Chem. Inf. Model.*, 2020, **60**, 2044–2058.

54 G. Landrum, RDKit: Open-Source Cheminformatics Software **https://github.com/rdkit/rdkit/releases/tag/Release_2016_09_4** 2016.

55 S. Riniker and G. A. Landrum, *J. Chem. Inf. Model.*, 2015, **55**, 2562–2574.

56 J. J. P. Stewart, *J. Mol. Model.*, 2013, **19**, 1–32.

57 M. J. Frisch, G. W. Trucks, H. B. Schlegel, G. E. Scuseria, M. A. Robb, J. R. Cheeseman, G. Scalmani, V. Barone, G. A. Petersson, H. Nakatsuji, X. Li, M. Caricato, A. V. Marenich, J. Bloino, B. G. Janesko, R. Gomperts, B. Mennucci, H. P. Hratchian, J. V. Ortiz, A. F. Izmaylov, J. L. Sonnenberg, D. Williams-Young, F. Ding, F. Lipparini, F. Egidi, J. Goings, B. Peng, A. Petrone, T. Henderson, D. Ranasinghe, V. G. Zakrzewski, J. Gao, N. Rega, G. Zheng, W. Liang, M. Hada, M. Ehara, K. Toyota, R. Fukuda, J. Hasegawa, M. Ishida, T. Nakajima, Y. Honda, O. Kitao, H. Nakai, T. Vreven, K. Throssell, J. A. Montgomery, Jr., J. E. Peralta, F. Ogliaro, M. J. Bearpark, J. J. Heyd, E. N. Brothers, K. N. Kudin, V. N. Staroverov, T. A. Keith, R. Kobayashi, J. Normand, K. Raghavachari, A. P. Rendell, J. C. Burant, S. S. Iyengar, J. Tomasi, M. Cossi, J. M. Millam, M. Klene, C. Adamo, R. Cammi, J. W. Ochterski, R. L. Martin, K. Morokuma, O. Farkas, J. B. Foresman and D. J. Fox, *Gaussian 16 (version Revision A.03)*, Gaussian, Inc., Wallingford CT, 2016.

This journal is © The Royal Society of Chemistry 2024

J. Mater. Chem. C, 2024, **12**, 13985–13993 | **13993**